Aeolian Research 12 (2014) 1–7

Contents lists available at ScienceDirect

Aeolian Research

journal homepage: www.elsevier.com/locate/aeolia

Investigation of the statistical features of sand creep motion with wind tunnel experiment

Yang Zhang, Yuan Wang *, Pan Jia

Department of Fluid Machinery and Engineering, Xi'an Jiaotong University, No. 28 Xianning Western Road, Xi'an 710049, China

ARTICLE INFO

Article history:
Received 11 January 2013
Revised 14 September 2013
Accepted 28 October 2013
Available online 17 November 2013

Keywords:
Aeolian sand creep motion
Wind tunnel experiment
High-speed photography
PTV
Intermittency of creep motion

ABSTRACT

A wind tunnel experiment has been adopted to investigate aeolian sand creep motion which has not been sufficiently documented thus far. An image sequence that describes continuous creep motion on a flat sand bed is recorded by high-speed photography, from which numerous creep trajectories are reconstructed by a particle tracking velocimetry (PTV) algorithm. A double-peak pattern present in the distribution of the starting velocity, which indicates the first stepping velocity of creep trajectory, is used to categorize all creep trajectories into flow- or collision-initiated groups. Increased friction velocity is shown to improve the proportion of collision-initiated creep motion. The proportion of the collision-initiated starting velocity against all stepping velocities increases with friction velocity; however, that of the flow-initiated starting velocity remains steady. These results indicate that a stronger wind intensifies the intermittency (the inverse of lifespan) of creep motion by converting it into saltation.

1. Introduction

Aeolian sand transport is a major contributor to landform change (Goudie et al., 2000) and creates environmental problems such as soil erosion and desertification (Pye, 1993). On the basis of pioneering research that indicates such transport begins with a single grain (Bagnold, 1941), classification of near-surface sand grain motion has been proposed and developed (Anderson et al., 1991; Andreotti et al., 2002) in which the importance of sand creep, i.e., the rolling or gliding of sand grains on a sand bed surface, has been repeatedly mentioned. However, most previous research has focused on saltation, in which sand grains are propelled in short hops. In such studies, sand creep was considered as either a factor in the formation of sand ripples (Wang and Hu, 2012) or as part of the overall sand flux (Dong et al., 2002; Wang and Zheng, 2004). In the present study, we view sand creep as independent surface granular flow (Khakhar et al., 2001; Aradian et al., 2002). For non-intrusive optical measurement, side-view photography with sheet-light illumination has been extensively applied to record saltation occurring in air (Nalpanis et al., 1993; Rice et al., 1996; Rice et al., 1999; Zhang et al., 2007). In contrast, top-view photography is the only method used to record creep motion because the creeping grains adhere to static sand beds. This method was originally used to study the diffusion transport of granular matter (Radice et al., 2006) and has been updated for use as an effective creep recording system (Wang et al., 2009).

Independent trajectories have been used to determine statistical features of grain motion for saltation (Zhang et al., 2007; Wang et al., 2008); however, this method has not been applied to creep thus far. The present study employs the aforementioned creep recording system and adopts a significantly longer sampling period to guarantee a sufficient sample size of creep trajectories, upon which a detailed statistical analysis is based.

2. Experimental

The present experiment was conducted in an open-type wind tunnel. Several roughness elements contained in a 10 m segment in the streamwise direction were installed upwind of the test section to simulate a thermally neutral atmospheric boundary layer (ABL). The reference wind speed U_0 was measured with a pitot tube located at the center of the wind tunnel entrance. The streamwise velocity profiles were measured separately using a particle imaging velocimetry system (Adrian, 1991). The measurement area was located on the central longitudinal section that is right above the sand bed, and the velocity profile was derived from the averaging of PIV velocity fields in the streamwise direction. As shown in Fig. 1, the maximum value of the streamwise turbulence intensity I_e located at the surface was approximately 25%. Within a thickness of about 0.25 m, the normalized velocity profiles were well-fitted by the logarithmic law:

$$U(z) = \frac{u^*}{\kappa} \ln\left(\frac{z}{z_0}\right), \tag{1}$$

* Corresponding author. Tel.: +86 2982663953; fax: +86 2982668723.
E-mail address: wangyuan@mail.xjtu.edu.cn (Y. Wang).

1875-9637/$ - see front matter © 2013 Elsevier B.V. All rights reserved.
http://dx.doi.org/10.1016/j.aeolia.2013.10.007

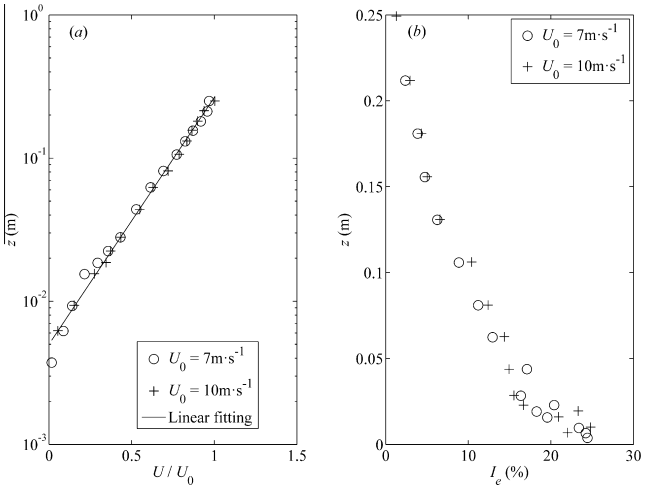

Fig. 1. Simulated atmospheric boundary layer: (a) streamwise mean velocity profile; (b) streamwise turbulence intensity.

where $U(z)$ is the mean streamwise velocity, z is the vertical distance above the surface, u_* is the friction speed, $\kappa \approx 0.42$ is the Karman constant, and $z_0 \approx 0.0048m$ is the effective roughness height. Near-surface sand motion generally occurred within 0.1 m above the surface. Therefore, sand movement in the simulated surface layer was similar to that under natural conditions.

The experimental and post-processing methods are illustrated in Fig. 2, and the experimental parameters are detailed in Table 1. The wind profile induced sand movement on the sand bed lain 5 m downstream of the entrance of the test section. Because creep motion occurs close to the bed surface, a high-speed camera was employed to capture movement from the top view. A very shallow depth of field (<1.5 mm) was obtained by adopting sufficiently large aperture and long focus (Meinhart et al., 2000), so that the saltating streaks appear blurred on the image and no longer possess the typical gray distribution calculated using a general cluster recognition algorithm (Ohmi and Li, 2000). In the present study, a shadowless illumination system composed of six halogen lights surrounding the test section was employed to eliminate the shadows projected by saltating streaks above the bed surface. The friction velocity u_* was altered to conduct six experimental runs, as shown in Table 1.

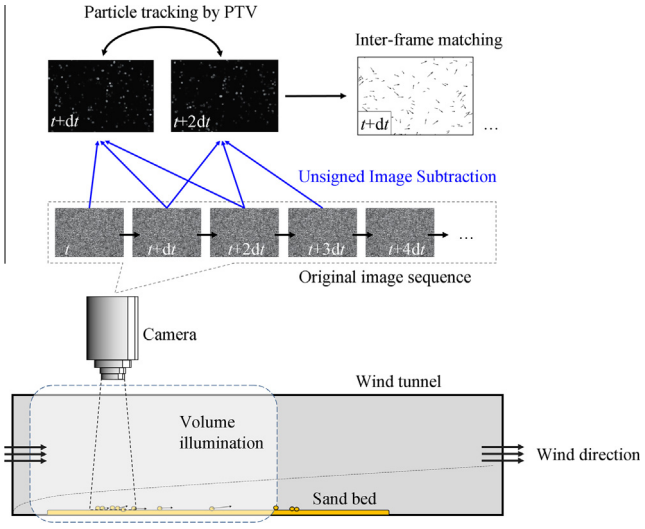

Fig. 2. Experimental setup and post-processing methods.

3. Reconstruction of creep trajectory

3.1. Recognition of creep sand grains

At moment i, the image I_i' that highlights the creep grains can be obtained with an algorithm known as unsigned image subtraction (UIS; Wang et al., 2009):

$$I_i' = \frac{(I_i - I_{i-1}) + |I_i - I_{i-1}| + |I_i - I_{i+1}| + (I_i - I_{i+1})}{4}, \quad (2)$$

where I_{i-1}, I_i, and I_{i+1} denote original images at three consecutive moments of $i-1$, i, and $i+1$, respectively. I_i' removes the static sand bed surface from the original image (Fig. 3) and preserves only moving blocks, as shown in Fig. 4a. The dynamical threshold binarization (DTB; Ohmi and Li, 2000) algorithm is next applied to I_i' to exclude saltating steaks exhibiting abnormal gray distribution. The creep grains appear as blocks composed of connected pixels. DTB identifies each block and replaces it with a single dot that corresponds to the geometric center of its pixels. In this process, the error scale is 0.1 pixels (Nicholas et al., 2006), which corresponds to 0.0025 m/s in our velocity result. This value is acceptable because the final creep velocity scale obtained was 0.1 m/s. The single dots representing instantaneous creep grain particles are then inputted into the particle tracking velocimetry algorithm (PTV; Uemura et al., 1989; Baek and Lee, 1996; Song et al., 1999).

3.2. Matching of inter-frame particles

PTV reconstructs continuous particle motion from a Lagrangian perspective. Specifically, this algorithm matches inter-frame single dots and reconstructs independent trajectories from a sequence of such matching relationships. The two-frame Delaunay-tessellation particle tracking velocimetry (DT–PTV, Song et al., 1999) algorithm is adopted in the present study because it is suitable for tracking discrete particles with random motion. In DT–PTV, particles on the same frame are combined to form a triangular colony (Fig. 4c), and the final inter-frame particle matching is determined through inter-frame triangle matching. The fundamental principle for PTV is that inter-frame particle displacement must be limited (Baek and Lee, 1996). The remaining streak-like saltating blocks that are not excluded by DTB cannot be matched under the framework of DTPTV because inter-frame displacement of saltating grains is excessively large compared with that of creep. Fig. 4d illustrates the inter-frame matching relationships presented by velocity vectors, in which the head and the end of vector correspond to two matched particles on the first and second frames, respectively.

4. Statistical features of creep trajectory

4.1. Distribution of starting velocity

From a creep trajectory containing N_t steps (or instants), a total of $N_t - 1$ stepping velocities can be obtained using the forward difference scheme (Zhang et al., 2007), in which the first stepping velocity is referred to as the starting velocity v_1 (Fig. 5). In each run, the starting velocities of all trajectories are collected to form a set $\{v_1\}$. The distributions of $\{v_1\}$ in all runs are shown in Fig. 6, in which a double-peak pattern can easily be identified.

A static sand grain can be dislodged into creep motion in either of two ways (Bagnold, 1941; Dong et al., 2010), as shown in Fig. 7. When u_* is merely adequate for overcoming the relative friction among sand grains, a grain is likely to be directly initiated driven by wind to roll on the surface, as shown in Fig. 7a. Such flow-initiated creep is denoted as c_1. With a larger u_*, additional grains